

# In situ Microwave Characterization of Nonplanar Dielectric Objects

Vasundara V. Varadan, *Member, IEEE*, K. A. Jose, and Vijay K. Varadan, *Member, IEEE*

**Abstract**—In this paper, a novel experimental solution is presented for the nondestructive, noncontact, and *in situ* characterization of dielectric objects of curved shape using a spot-focused free-space measurement system. Measurements were made on Plexiglas and glass samples of cylindrical shape with different radii of curvature, and the complex permittivities were computed from the measured  $S_{21}$  and  $S_{12}$ . Comparing the results with planar samples show that the curvature does not significantly affect the accuracy of the measured permittivity of cylindrical surfaces if the radii of curvature are large compared to the size of the focusing spot. Results for a number of curved samples agree with the published data and this demonstrates the usefulness of a spot-focused free-space system for *in situ* characterization and evaluation of materials and complex structures during processing and fabrication. The other benefit of this approach is the noncontact nature of the method, which permits measurement of solids and liquids in high-/low-temperature environments. The spot-focused beam permits characterization of small or large samples.

**Index Terms**—Dielectric measurement, free-space method, microwave nondestructive testing, permittivity measurement.

## I. INTRODUCTION

RECENT material technologies offering lighter, stronger, and more durable composites require new inspection methods for quality control during the manufacturing process and for health monitoring during service. Different methods for microwave nondestructive testing (NDT) and evaluation of dielectric samples have been employed for many years [1]–[3]. Microwaves can penetrate deeper into dielectric materials in contrast to ultrasound. The different propagation properties of microwaves at different media can be applied for thickness measurements [4], evaluation of sandwich composites [5], flaw/defect detection [6], [7] strength estimation of cements [8], and monitoring the curing conditions [9]. However, these methods are qualitative and require large samples or contact measurements. A review of common methods for nondestructive permittivity and permeability evaluation is presented in [10] and [11]. The introduction of spot-focused antennas introduced by Varadan *et al.* [12]–[16] permit focused plane wave illumination of samples in a noncontact manner. Using thru-reflect line (TRL) calibration, this technique has been used to accurately measure the complex permittivity, complex permeability, and chiral properties of novel microwave composite materials as a function of frequency and temperature using

both normal and obliquely incident waves. Later, Al-Qudi *et al.* [17] presented a useful application of this technique for the noncontact nondestructive measurement of moisture content of asphaltic cements.

Most of the classical methods of permittivity measurements require special preparation of a sample in order to fit into the waveguide sample holder or cavity resonator. Open-ended coaxial probes offer some promise in nondestructive applications. In such measurements, the coaxial probe should be pressed against the dielectric sample and the measured reflection coefficient is used to compute its permittivity. However, the contact between the sample and probe is most important and a small discontinuity in the normal electric field can cause a large error in the measured permittivity. Bringhurst *et al.* [18] established that, for a 1.0-mm air gap in between the inner conductor and sample, there is a chance of up to 80% error in  $\epsilon'$  and  $\epsilon''$  for alumina sample. The coaxial measurement technique is suitable only for the planar samples or for samples in liquid form. An alternate method for permittivity measurements using radiating horns in free space requires samples in sheet form that have transverse dimensions much larger than the wavelength (Naval Research Laboratory arch method). There is a pressing need for techniques that permits *in situ* microwave material characterization of nonplanar or cylindrical materials. Such references are lacking in the literature.

Chan and Chambers [19] describe an open resonator technique for evaluation of complex permittivity of curved samples at 11.6 GHz. The Gaussian beam between two mirrors in a cavity resonator forms standing-wave pattern and the curvature of the wavefront varies along the axis of the resonator. In this configuration, convex-concave samples are measured at off-center positions inside the resonator where wavefronts are curved and similar in form of the sample surfaces. When sample surfaces are approximately coincident with the wavefronts, experimental errors are mainly due to uncertainties in the measurement of sample geometry, sample position, resonant frequency, and  $Q$  factor. In this technique, the sample is not required to be positioned at a particular point within the resonator, but a full description of sample geometry is needed. Being a resonance method, it is confined to a single frequency.

The need to measure samples with very small transverse dimension is addressed by the focused beam antennas [12]–[16]. Previously, this approach has been used for the accurate measurement of electromagnetic (EM) properties of planar samples of composite materials, anisotropic composites, and chiral composites. The advantage of this method is that the same physical sample can be measured over a wide frequency span, unlike waveguide or coaxial methods that require a sample to be fitted

Manuscript received October 9, 1998; revised December 10, 1999.

The authors are with the Center for the Engineering of Electronic and Acoustic Materials, Department of Engineering Science and Mechanics, Pennsylvania State University, University Park, PA 16801 USA.

Publisher Item Identifier S 0018-9480(00)02068-8.

into a fixture for each band. Being a noncontact method, it is well suited for quick and routine evaluation of broad-band material characteristics as a function of temperature [14]. In this paper, we demonstrate the efficiency of the free-space system for *in situ* material property characterization of nonplanar dielectric samples. The dielectric constant and loss tangent of the nonplanar specimens were computed from the measured complex transmission or reflection coefficients. This may find wide application for *in situ* microwave characterization of liquids and solids during processing and for inspecting fabricated parts such as radomes, microwave lenses, and EM coatings.

## II. THEORY

This method for determining complex permittivity in free space is based on the accurate measurement of the transmission coefficient  $S_{21}$  through the sample and/or the reflection coefficient  $S_{11}$  from the front face of the curved sample. The simplest model considers a plane EM wave incident normally on a planar slab of infinite homogeneous dielectric medium. The measured reflection coefficients  $S_{11}$  and transmission coefficients  $S_{21}$  are related to the parameters  $\Gamma$  and  $T$  by [12]

$$S_{11} = \frac{\Gamma(1 - T^2)}{1 - \Gamma^2 T^2} \quad (1)$$

$$S_{21} = \frac{T(1 - \Gamma^2)}{1 - \Gamma^2 T^2}. \quad (2)$$

The reflection and transmission coefficients  $\Gamma$  and  $T$  are given as

$$\Gamma = \frac{(Z_{sn} - 1)}{(Z_{sn} + 1)} \quad (3)$$

$$T = e^{-\gamma d}. \quad (4)$$

$Z_{sn} = (1/\sqrt{\epsilon^*})$  and  $\gamma = k_0 (\epsilon^*)^{1/2}$  are the normalized characteristic impedance and propagation constant of the sample,  $k_0 = (2\pi/\lambda_0)$ ,  $\lambda_0$  is the wavelength in free space, and  $d$  is the thickness of the sample. The dielectric properties can be calculated from

$$\epsilon^* = \frac{\gamma}{\gamma_0} \left( \frac{1 - \Gamma}{1 + \Gamma} \right) \quad (5)$$

The measurement system is calibrated at a reference plane at the focus of the antennas and the samples are placed at that point, as shown in Fig. 1. The inversion of the measured data is prone to errors if there are uncertainties in the orientation of the sample with respect to the calibration plane. It is evident that the  $S_{11}$  measurements are more prone to error due to the dependence of the reflected signal on the phase of the incident signal at the sample front face. However,  $S_{21}$  depends on the path length, which is independent of the sample position relative to the reference plane. Using the time-domain gating facility of the Network Analyzer eliminates the multiple reflected signals between the sample and antenna. The relative permittivity ( $\epsilon_r^* = \epsilon_r' + j\epsilon_r''$ ) can be computed from the measured values of  $S_{21}$ . It is assumed that the sample is nonmagnetic, i.e.,  $\mu^* = I +$

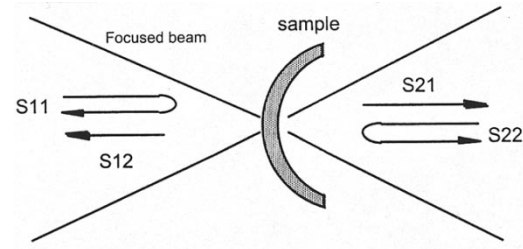


Fig. 1. Free-space spot-focused measurement configuration.

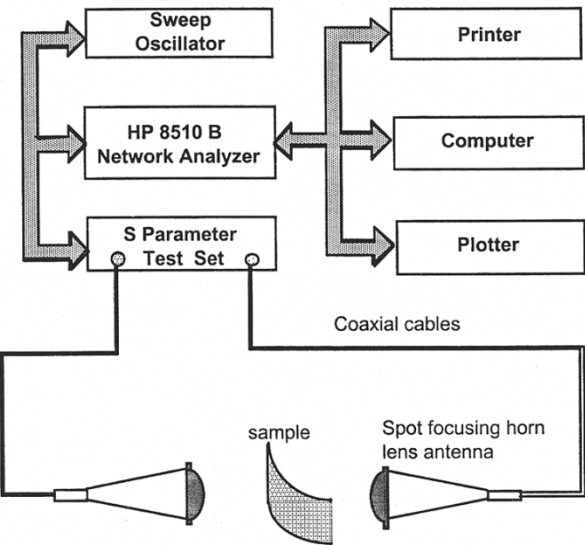
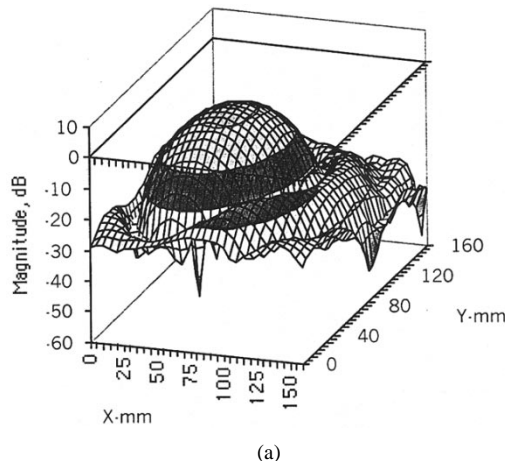


Fig. 2. Schematic diagram of the free-space dielectric-constant measurement setup for the nonplanar samples.

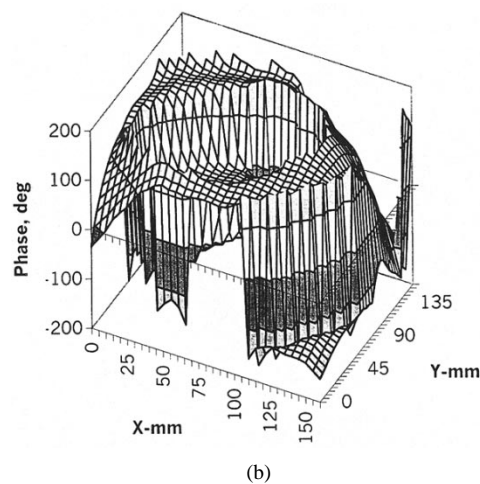
0. From (2) and the definitions that follow, it is possible to obtain  $S_{21}$  in terms of  $\epsilon^*$ . However, the exact solution for  $\epsilon^*$  is not straightforward due to the multiple roots for (3). Hence, an iterative technique using an initial guess for the  $\epsilon^*$  is used. The initial guess is obtained from the estimated value of the phase velocity in the sample computed from the difference in phase at the measurement plane without and with a sample [14].

## III. EXPERIMENTAL TECHNIQUES

A schematic diagram of the experimental setup is shown in Fig. 2. The instrumentation system consists of a vector network analyzer connected to lens-focused horn antennas via coaxial cables and coax to waveguide transitions. The data from the network analyzer is downloaded to a computer for processing and inversion. The spot-focusing horn lens antenna consists of two equal plano convex dielectric lenses mounted back to back at the aperture of a horn antenna. The antennas are mounted facing each other and a sample holder is placed at a common focal plane of the two antennas. Due to the spot focusing of the lens antennas, the diffraction effects due to the edges of the sample are negligible if the sample dimension is greater than three times the  $E$ -plane 3-dB beamwidth [13]. The measurement system is calibrated using free-space TRL calibration and error-correction technique [12], [13]. The TRL technique requires three standards, namely, a through connection, short connected to each port, and line connected between the test ports



(a)



(b)

Fig. 3. (a) Measured amplitude map at the focus of the spot-focused horn antenna at 9.1 GHz. (b) Measured phase map at the focus of the spot-focused horn antenna at 9.1 GHz.

with a known delay. Compared to other coax or waveguide calibration standards, the TRL standards are easy to implement. In free-space TRL calibration, the **thru** connection is realized by keeping the distance between two antennas equal to twice the focal distance. The **reflect** standards for ports 1 and 2 are obtained by mounting a highly polished plane metal plate at the reference plane. The **line** standard is achieved by introducing a separation between the focal planes of two antennas, which is usually quarter-wavelength at midband. After calibration, the **thru** connection ( $S_{21}$  and  $S_{12}$ ) measured was with amplitude within  $\pm 0.25$  dB and phase  $\pm 1.0^\circ$  and magnitude of  $S_{11}$  and  $S_{22}$  was less than  $-50$  dB. In a manufacturing environment, the implementation of free-space TRL calibration is quite easy because **thru** and **line** standards require only change in antenna positions.

The phase distribution of the focused beam at the focus is very important for the permittivity measurement of the non-planar samples. The phase distribution gives information about the character of the wavefront at the focus. To check the spot-focusing nature of the antenna, the amplitude and phase of the field at the focus of the antenna were mapped and are presented in Fig. 3(a) and (b). It can be seen from the field distribution that the beam has a character of plane wave at the focus and the mea-

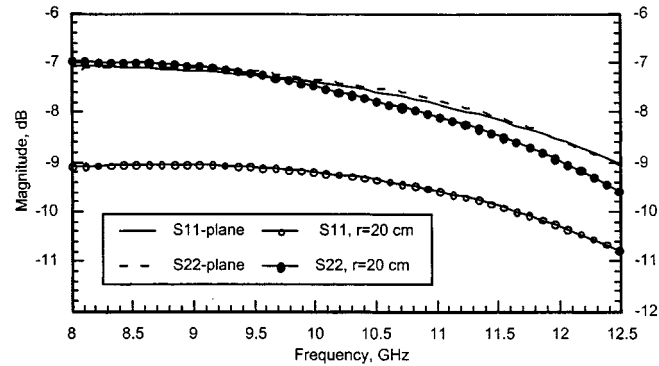


Fig. 4. Comparison of magnitude of measured  $S_{11}$  and  $S_{22}$  for plane and curved (radius of curvature = 20 cm) Plexiglas sample of thickness 0.53 cm.

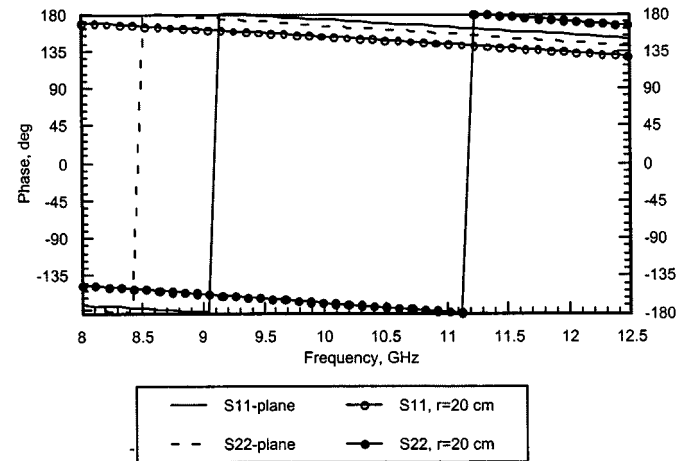


Fig. 5. Comparison of measured phase of  $S_{11}$  and  $S_{22}$  for plane and curved (radius of curvature = 20 cm) Plexiglas sample of thickness 0.53 cm.

sured  $-3$ -dB spot size of the focused beam is  $4.37$  cm  $\times$   $3.2$  cm. The focal length is  $30.5$  cm, measured from the aperture of the antenna and it has a focal depth of  $8.4$  wavelengths at  $10$  GHz. The plane-wave character is evident at the center of the map and the variation of the phase at the center at  $-3$ -dB region is  $3.50$ .

#### IV. RESULTS AND DISCUSSIONS

$S$ -parameter measurements were made on planar as well as curved samples of the same wall thickness. Using the two spot-focused horn antennas, forward ( $S_{21}$ ) and reverse ( $S_{12}$ ) transmission coefficients, as well as reflection ( $S_{11}$ ) from the convex surface and reflection ( $S_{22}$ ) from the concave surface were measured. These results were used for the computation of the dielectric constant of the curved samples. The samples were made by cutting  $15$  cm  $\times$   $15$  cm pieces from circular cylinders of radii  $50$ ,  $40$ ,  $30$ ,  $20$  and  $10$  cm, respectively. Curved samples of Plexiglas and glass with different radii of curvatures were measured and the results are compared with respective planar samples of the same thickness.

In Figs. 4–7, the magnitude and phase of the measured  $S_{11}$  and  $S_{22}$  reflection coefficients and  $S_{21}$  and  $S_{12}$  transmission coefficients for a Plexiglas sample of radius of curvature of  $20$  cm and thickness  $0.53$  cm are compared with planar sample of the same thickness. It is clear from the figure that the reflections

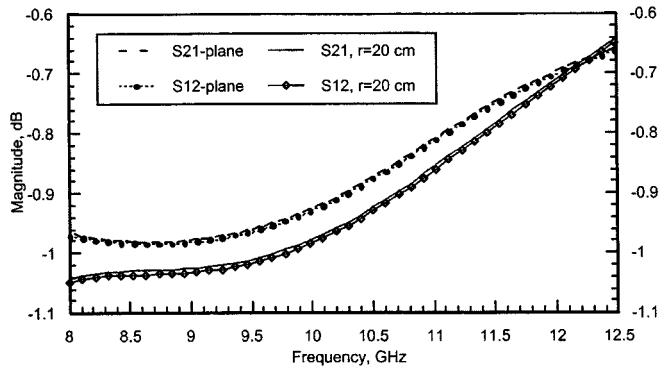


Fig. 6. Comparison of magnitude of measured  $S_{21}$  and  $S_{12}$  for plane and curved (radius of curvature = 20 cm) Plexiglas samples of thickness 0.53 cm.

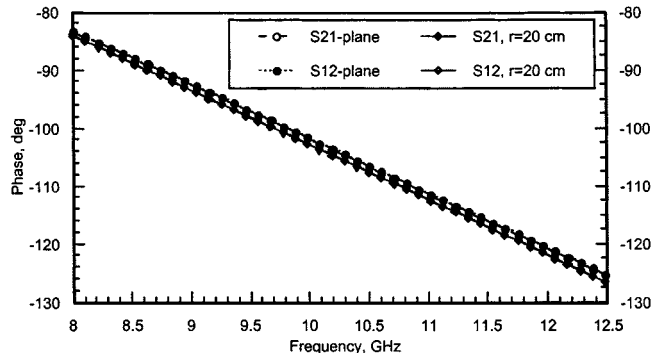
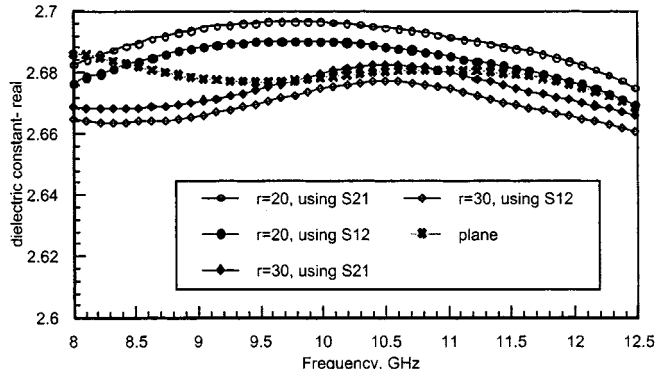


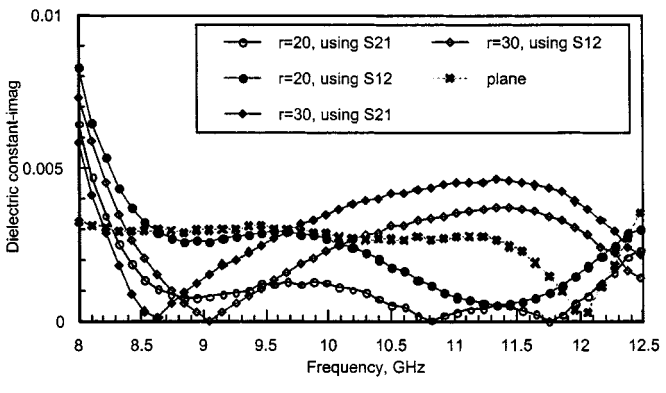
Fig. 7. Comparison of measured phase of  $S_{21}$  and  $S_{12}$  for plane and curved (radius of curvature = 20 cm) Plexiglas sample of thickness 0.53 cm.

from convex and concave surfaces are different due to curvature. The focused antenna is able to pick up more of the reflected field from the concave than from the convex surface, which may reflect signals outside the receiving aperture of the lens. For the plane sample, both faces are identical and it can be seen that the magnitude of the reflection coefficient  $S_{22}$  from the concave face agrees very well with the plane sample, whereas the  $S_{11}$  from the convex side is about 2 dB less over the entire frequency range, indicating that the antenna lens is not picking up all of the reflected field. Even for the concave face, as the frequency increases, there is a small deviation from the planar sample result. The phase of the reflected field is more sensitive to the curvature, as can be seen from Fig. 5, where there are significant differences between curved and planar samples as well as the convex and concave faces of the sample. From Figs. 5 and 6, it may be concluded that inversion of material properties from reflection data for curved samples treating them as locally planar in the illuminated spot will lead to large errors. Corrections will have to be effected for the effect of curvature. This is deferred to a later paper.

Fig. 6 presents a comparison of the magnitude of  $S_{21}$  and  $S_{12}$  for curved and planar samples. In Fig. 7, a comparison of phase data is presented. From Figs. 6 and 7, we observe that the focused antennas receive all of the transmitted power from both convex and concave faces of the sample and, further, there is very agreement between the planar and curved sample results. Thus, inversion of the transmission data for the complex permittivity of the sample is very promising. It is also noted from



(a)



(b)

Fig. 8. (a) Real part of the complex permittivity as a function of frequency inverted using  $S_{21}$  and  $S_{12}$  for Plexiglas of radii of curvature 20 cm, 30 cm, and the planar sample. (b) Imaginary part of the measured complex permittivity as a function of frequency for Plexiglas of radii of curvature 20 cm, 30 cm, and the plane sample.

Fig. 7 that the phase of the field transmitted through the curve sample is very linear with frequency, indicating that the thickness of the sample can be determined using this approach if the dielectric property is known.

The complex permittivities were calculated by inverting the measured  $S_{21}$  and  $S_{12}$  and are presented in Fig. 8(a) and (b) for samples of radii of curvature 20 and 30 cm, and are compared with corresponding planar samples of the same thickness. The deviation of the measured value of relative permittivity from the actual value due to the curvature varying from 50 to 20 cm, in the present study, is 1.8% for the Plexiglas sample. It may be noted that the samples were cut from cylinders having different radii of curvature and the material properties of the cylinders may vary from cylinder to cylinder due to manufacturing problems. It is evident from Fig. 8 that the curvature effect is negligible for computation of permittivity using transmission measurements treating the sample as locally planar. This assumption appears to hold well even for the lowest radius of curvature of 20 cm, which is, however, larger than wavelengths in  $X$ -band. Table I presents the summary of the measured complex permittivity of five samples of Plexiglas of different radii of curvature for different frequencies. The reported results of the plexiglas samples using the open resonator method [19] are shown in Table II for comparison purposes.

TABLE I  
MEASURED PERMITTIVITIES FOR DIFFERENT RADII OF CURVATURE OF PLEXIGLAS SAMPLES USING SPOT-FOCUSED FREE-SPACE SYSTEM

| Freq.<br>GHz | Measured permittivities of Plexiglas (different radii of curvature) |               |             |               |             |               |             |               |             |               |
|--------------|---|---------------|-------------|---------------|-------------|---------------|-------------|---------------|-------------|---------------|
|              | Plane   |               | r= 50 cm    |               | r=40 cm     |               | r=30 cm     |               | r=20 cm     |               |
|              | $\epsilon'$   | $\tan \delta$ | $\epsilon'$ | $\tan \delta$ | $\epsilon'$ | $\tan \delta$ | $\epsilon'$ | $\tan \delta$ | $\epsilon'$ | $\tan \delta$ |
| 8.008        | 2.6848  | 0.0030        | 2.6842      | 0.0060        | 2.6814      | 0.0074        | 2.6875      | 0.0040        | 2.6792      | 0.0071        |
| 8.320        | 2.6818  | 0.0029        | 2.6816      | 0.0055        | 2.6788      | 0.0071        | 2.6854      | 0.0001        | 2.6822      | 0.0031        |
| 8.736        | 2.6784  | 0.0029        | 2.6803      | 0.0044        | 2.6775      | 0.0072        | 2.6851      | 0.0027        | 2.6858      | 0.0009        |
| 9.152        | 2.6770  | 0.0031        | 2.6807      | 0.0055        | 2.6790      | 0.0080        | 2.6880      | 0.0040        | 2.6897      | 0.0003        |
| 9.568        | 2.6773  | 0.0029        | 2.6829      | 0.0061        | 2.6819      | 0.0081        | 2.6924      | 0.0045        | 2.6920      | 0.0008        |
| 9.984        | 2.6791  | 0.0027        | 2.6856      | 0.0063        | 2.6857      | 0.0076        | 2.6970      | 0.0043        | 2.6922      | 0.0016        |
| 10.400       | 2.6804  | 0.0026        | 2.6862      | 0.0060        | 2.6974      | 0.0069        | 2.6987      | 0.0039        | 2.6900      | 0.0020        |
| 10.816       | 2.6808  | 0.0027        | 2.6842      | 0.0059        | 2.6857      | 0.0062        | 2.6967      | 0.0037        | 2.6858      | 0.0017        |
| 11.232       | 2.6797  | 0.0024        | 2.6801      | 0.0061        | 2.6819      | 0.0057        | 2.6925      | 0.0039        | 2.6811      | 0.0009        |
| 11.648       | 2.6772  | 0.0020        | 2.6767      | 0.0060        | 2.6784      | 0.0044        | 2.6865      | 0.0039        | 2.6775      | 0.0062        |
| 12.064       | 2.6722  | 0.0018        | 2.6747      | 0.0047        | 2.6761      | 0.0024        | 2.6855      | 0.0029        | 2.6735      | 0.0014        |
| 12.480       | 2.6637  | 0.0021        | 2.6722      | 0.0062        | 2.6725      | 0.0024        | 2.6809      | 0.0012        | 2.6672      | 0.0029        |

TABLE II  
MEASURED PERMITTIVITIES OF PLEXIGLAS FOR PLANE AND CURVED SAMPLES USING OPEN RESONATOR METHOD BY CHAN AND CHAMBERS [19]

| Freq.<br>GHz  | Permittivities of Perspex (plexiglas) measured for flat and convex-concave samples by<br>Chan and Chambers [19] |          |          |          |         |         |         |         |         |
|---------------|---|----------|----------|----------|---------|---------|---------|---------|---------|
|               | plane   | 560.3 cm | 249.7 cm | 140.2 cm | 87.4 cm | 64.8 cm | 48.8 cm | 38.6 cm | 33.0 cm |
| 11.59         |   |          |          |          |         |         |         |         |         |
| $\epsilon'$   | 2.611   | 2.628    | 2.628    | 2.627    | 2.629   | 2.631   | 2.590   | 2.582   | 2.581   |
| $\tan \delta$ | 0.0059  | 0.0070   | 0.0069   | 0.0069   | 0.0069  | 0.0070  | 0.0043  | 0.0041  | 0.0043  |

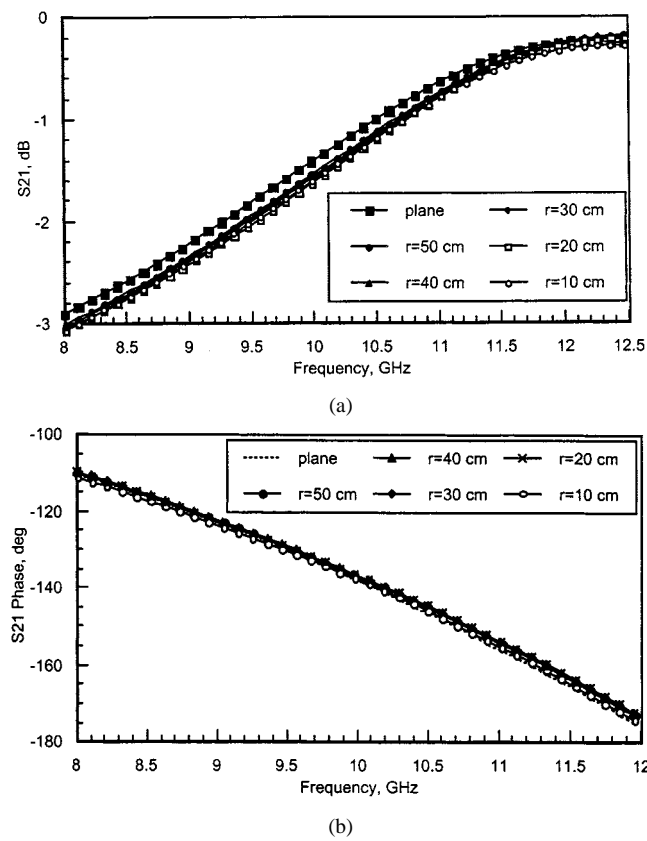
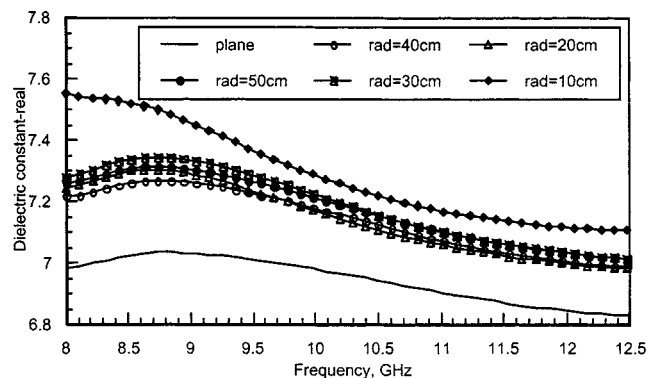


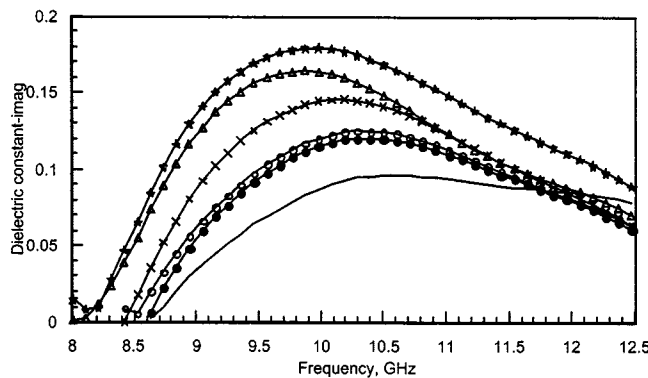
Fig. 9. (a) Comparison of magnitude of  $S_{21}$  measured as a function of frequency for five glass samples of radii of curvature 50 to 10 cm with a plane sample of same thickness (0.46 cm). (b) Comparison of measured phase of  $S_{21}$  as a function of frequency for five glass samples of radii of curvature 50 to 10 cm with a plane sample of the same thickness (0.46 cm).

In Fig. 9(a) and (b), we present the measured  $S_{21}$  magnitude and phase of the curved glass sample of thickness 0.46 cm for different radii of curvature from 10 to 50 cm, and compare them to a plane sample of same thickness. The real and imaginary parts of the complex dielectric permittivity are computed using measured  $S_{21}$ , and are presented in Fig. 10(a) and (b). Again, there is excellent agreement with results for the planar sample even for a radius of curvature of 10 cm, which is approximately  $3\lambda$  at mid-band.

The accuracy of the measurements of nonplanar dielectric materials using the free-space setup depends mainly on the precise alignment of the geometric center of the cylindrical sample with the axis of the antenna system. Measurements were made to estimate how the errors in the measurement of  $S_{21}$  could affect the permittivity by off-centering the geometric center of the cylinder to different positions away from the initial position. This is, in effect, keeping the sample at the same distance and moving its center laterally to different positions. Fig. 11(a) and (b) presents the percentage error in the measured permittivities for different off-centered positions of the sample. It is observed that by moving the geometric center about 5.04 cm, the real part of the dielectric constant has an inconsistency of about 2% to that of its actual value. However the  $\tan \delta$  is found to be more sensitive to the position of the sample. This leads to the conclusion that for accurate permittivity measurements of the nonplanar samples using a spot-focused free-space system, the unit normal of the center of the illuminated spot on the sample should be aligned with the axis of the antenna system.



(a)

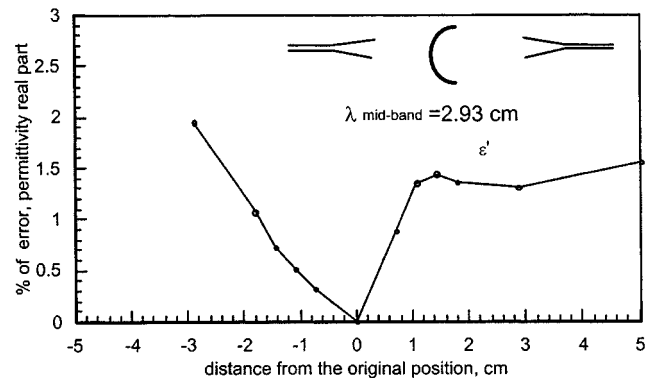


(b)

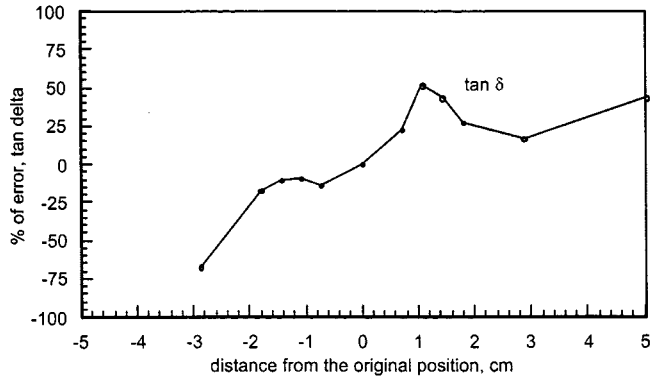
Fig. 10. (a) Real part of the measured complex permittivity versus frequency for six curved glass samples of different radii of curvature: thickness 0.46 cm and a plane sample. (b) Imaginary part of the measured complex permittivity versus frequency for six curved glass samples of different radii of curvature: thickness 0.46 cm.

## V. CONCLUSIONS

Most of the existing techniques for the characterization of materials are applicable only to planar samples or specimens shaped to fit into the measurement devices. Measurements of the electrical properties of planar samples are quite accurate using the spot-focused free-space measurement system. In this paper, we have demonstrated the efficiency of the spot-focused free-space measurement system for the nondestructive and *in situ* evaluation of dielectric properties of curved samples in a noncontact mode. Measured results for curved Plexiglas and glass and comparison to a corresponding planar sample demonstrate that accurate results can be obtained provided the curved surfaces have radii of curvature larger than the focusing spot of the antenna. The measured spot size of the antenna at  $-3$  dB power level is  $4.3 \text{ cm} \times 3.2 \text{ cm}$  in the  $X$ -band. It is possible to evaluate the material properties from 5 to 40 GHz using the present free-space measurement facility. For brevity, we have presented only the results of  $X$ -band measurements in this paper. The error analysis has been done to prove that errors in the positioning of



(a)



(b)

Fig. 11. (a) Percentage change of the real part of the permittivity by off-centering the sample from its geometric center: radius = 20 cm, thickness = 0.53 cm. (b) Percentage change of  $\tan \delta$  by off-centering the sample from its geometric center: radius = 20 cm, thickness = 0.53 cm.

the sample can contribute to errors in the inverted complex permittivity. The resulting errors are larger for the loss tangent. It is also shown that transmission measurements can be used to infer the thickness of curved samples very accurately in a noncontact manner. Further research is being pursued to explore applications of thickness measurements of solid and liquid films as a function of frequency and temperature.

In this paper, we have presented a practical user-friendly method for characterizing nonplanar dielectric materials with radii of curvature greater than the spot size of the focused beam. Further investigations can reveal the limitations of this approach to objects of more complex shape and smaller radii of curvature. It would be possible to measure the permittivities of samples of any radii of curvature by applying a curvature correction for the transmission coefficient, and this will be presented in the future. This technique should find wide applications in industry for *in situ* material characterization and health monitoring of parts in service.

## ACKNOWLEDGMENT

The antenna field mapping facility at HVS Technologies, State College, University Park, PA, is acknowledged. The authors wish to thank A. Tellakula for help with the antenna field mapping.

## REFERENCES

- [1] A. J. Bhar, *Microwave Nondestructive Testing Methods*. New York: Gordon and Breach, 1982.
- [2] R. Zoughi and S. Ganchev, *Microwave Nondestructive Evaluation: State-of-the-Art Review*. Austin, TX: Nondestructive Testing Inform. Analysis Center, 1995.
- [3] N. Ida, *Microwave NDT*. New York: Academic, 1992.
- [4] R. Zoughi and M. Lujin, "Nondestructive microwave thickness measurement of dielectric slabs," *Materials Evaluation*, vol. 48, pp. 1100-1105, Sept. 1990.
- [5] S. I. Ganchev, R. J. Runser, N. Qaddoumi, E. Ranu, and G. Carriveau, "Microwave nondestructive evaluation of thick sandwich composites," *Mater. Eval.*, pp. 463-467, Apr. 1995.
- [6] C. Y. Yeh and R. Zoughi, "Sizing techniques for slots and surface cracks in metals," *Mater. Eval.*, vol. 53, pp. 496-501, 1995.
- [7] J. Kurian, K. A. Jose, K. G. Balakrishnan, and K. G. Nair, "Microwave nondestructive flaw/defect detection system for non-metallic media supported by microprocessor based instrumentation system," *J. Microwave Power Electromag. Energy*, vol. 24, no. 2, pp. 74-78, 1989.
- [8] W. Shalaby and R. Zoughi, "Microwave composite strength estimation of cement paste using monopole probes," in *Research in Nondestructive Evaluation*. Berlin, Germany: Springer-Verlag, 1995, vol. 7, pp. 101-106.
- [9] K. A. Jose, P. Venugopalan, K. G. Nair, U. R. Ravindran, and P. K. Chathurvedi, "Microwave method for monitoring the curing conditions of a solid rocket propellant," *NDT Int.*, pp. 398-400, Dec. 1986.
- [10] J. Baker-Jarvis, C. Jones, B. Riddle, M. Janezic, R. C. Geyer, J. H. Grosvenor, Jr., and C. M. Weil, "Dielectric and magnetic measurements: A survey of nondestructive, quasi-nondestructive and process control techniques," in *Research in Nondestructive Evaluation*. Berlin, Germany: Springer-Verlag, 1995, vol. 7, pp. 117-130.
- [11] R. Zoughi, "Microwave and millimeter wave non-destructive testing: A succinct review," *Mater. Eval.*, vol. 53, pp. 461-462, 1995.
- [12] D. K. Thodgaonkar, V. V. Varadan, and V. K. Varadan, "A free space method for measurement of dielectric constant and loss tangent at microwave frequencies," *IEEE Trans. Instrum. Meas.*, vol. 37, pp. 789-793, June 1989.
- [13] —, "Free space measurement of complex permittivity and complex permeability of magnetic materials at microwave frequencies," *IEEE Trans. Instrum. Meas.*, vol. 39, pp. 387-394, Apr. 1990.
- [14] V. V. Varadan, R. D. Hollinger, D. K. Gahodganonkar, and V. K. Varadan, "Free space broad-band measurement of high temperature complex dielectric properties at microwave frequencies," *IEEE Trans. Instrum. Meas.*, vol. 40, pp. 842-846, May 1991.
- [15] M. H. Umari, D. K. Ghodgaonkar, V. V. Varadan, and V. K. Varadan, "A free space bistatic calibration technique for the measurement of parallel and perpendicular reflection coefficients of planar samples," *IEEE Trans. Instrum. Meas.*, vol. 40, pp. 19-24, Jan. 1991.
- [16] V. V. Varadan, R. Ro, and V. K. Varadan, "Measurement of electromagnetic properties of chiral composite materials in the 8-40 GHz range," *Radio Sci.*, vol. 29, pp. 9-22, 1994.
- [17] I. L. Al-Qadi, D. K. Ghodgaonkar, V. K. Varadan, and V. V. Varadan, "Effect of moisture on Asphaltic concrete at microwave frequencies," *IEEE Trans. Geosci. Remote Sensing*, vol. 29, pp. 710-717, Sept. 1991.
- [18] S. Bringhurst, M. F. Iskander, and M. J. White, "Thin sample measurements and error analysis of high temperature coaxial dielectric probes," *IEEE Microwave Theory Tech.*, vol. 45, pp. 2073-2083, Dec. 1997.
- [19] W. F. P. Chan and B. Chambers, "Measurement of nonplanar dielectric samples using an open resonator," *IEEE Trans. Microwave Theory Tech.*, vol. MTT-35, pp. 1429-1434, Dec. 1987.

**Vasundara V. Varadan** (M'82) received the Ph.D. degree from the University of Illinois at Chicago, in 1974.

She is currently an Alumni Distinguished Professor of engineering science and electrical engineering in the Department of Engineering Science and Mechanics, Pennsylvania State University, University Park. Her research interests include free-space microwave materials characterization methods, microwave nondestructive evaluation (NDE), health monitoring, chiral microwave absorbers, wireless SAW sensors, microelectromechanical systems (MEMS), and numerical modeling.



**K. A. Jose** received the Ph.D. degree from the Cochin University of Science and Technology, Cochin, India, in 1989.

After serving on the faculty of Cochin University from 1990 to 1997, he joined the Center for the Engineering of Electronic and Acoustic Materials, Pennsylvania State University, University Park, where he is currently a Senior Research Associate. His current research interests include microwave material characterization, RF wireless sensors, and smart antennas.

**Vijay K. Varadan** (M'82) received the Ph.D. degree from Northwestern University, Evanston, IL, in 1974.

He is currently an Alumni Distinguished Professor of engineering science and electrical engineering in the Department of Engineering Science and Mechanics, Pennsylvania State University, University Park. He is currently the Editor-in-Chief of the *Journal of Smart Materials and Structures*. His research interests include microwave materials, fractal antennas, tunable dielectrics, MEMS, wireless RF microgyros, and stereo microlithography.